Time Delay Spatial Patterns in 2D Array of Coupled Oscillators

By Jeong et. al., replicated by Brianna Marsh and Lawson Fuller
March 25, 2020

Abstract

We replicate results previously attained by Jeong et al. [1] for figures 4a and 4b and include results using new parameter configurations. In the interest of slightly more realism, we introduce sparsity for those sets of parameters and include those results. We find that interesting patterns still sometimes manifest for sparse connections and sometimes do not occur.

1 Introduction

Oscillatory properties of neurons have been studied in many different contexts and likely encode much behaviorally relevant information (Muller et al., 2018 [2]). In biological neural networks, there are many different types of neurons with complicated patterns of connectivity (often dense local connections and sparse distant connections), differences in speed of communication via differences in axon diameter and myelination, different chemical receptors and signals, and the list goes on.

As in the paper by Jeong et al. [1], we represent densely connected neural network with a network of coupled oscillators on a 2-D plane with periodic boundary conditions. The grid of coupled oscillators studied here is a much simplified version of a biological neural network in which every neuron (oscillator) has the same speed of communication to every other neuron within a certain radius. These simplifications provide a starting point to investigate general properties of interactions between coupled oscillators.

The paper by Jeong et al. saw many types of planar rolls and spirals appearing in their simulations. Despite many complications to the setup, such patterns have also been seen in biological neural networks such as the turtle visual cortex, rabbit olfactory cortex, and widely across human cortex (Ermentrout and Kleinfeld, 2001 [3]).

Such spatial patterning is relevant to not only healthy neural networks, but also diseased networks. Lainscsek et al. (2019) [4] showed the utility of a method called Delayed Differential Analysis (DDA) in detecting seizures; in one patient, all 7 recorded seizures could be predicted up to 2 hours before the event using this method (figure 1 below). DDA shows that the seizures are predicted by chimera states, in which the parts of the brain identified by the clinician to be the onset of the seizure (channels 1-30 below) show different levels of synchrony than the rest of the brain preceding each of the 7 seizures.

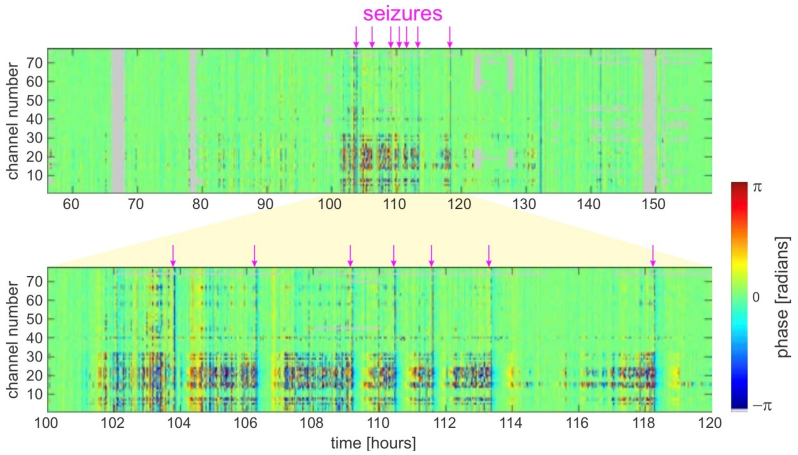

Figure 1: Prediction of seizures

The authors of this review suppose that, if properly visualized, the onset channels might show unique spatial patterns during this chimera state. One crucial component of the DDA algorithm is choosing two time delays to use in the equations; choosing proper time delays is a non-trivial task. Finding time delays that mimic those spatial patterns in a grid of coupled oscillators may give insight into the best time delays to use to find these chimera states in epileptic patients and predict seizure onset.

2 The Equation and Computation

Let $\theta_{i,j}$ denote an oscillator with phase θ in the i^{th} row and j^{th} column. The oscillator at location (i, j) experiences a phase rate of change $\dot{\theta}_{ij}$:

$$\dot{\theta}_{ij}(t) = w + \frac{K}{N(r_0)} \Sigma_{k,l}^{0<r_{kl,ij}<r_0} W(r_{kl,ij}) \times sin\big[\theta_{kl}\big(t - \frac{r_{kl,ij}}{v}\big) - \theta_{ij}(t)\big]$$

The term w is an internal rate common to all oscillators. The summation is over all locations (k, l) within a radius r_0 of (i, j). The sine in the summation has the effect of drawing θ_{ij} closer to the observed (time-delayed) θ_{kl} of its neighbors. If there were no time delay and only two oscillators, this sine term would attempt to synchronize the two oscillators.

It is critical that the algorithm runtime usage scales reasonably slowly with grid size to allow large numbers of oscillators and therefore interesting and easily identifiable dynamics. Calculating the weights W_{ijkl} in a nested for loop is time-inefficient, so we exploited the redundancy inherent in the translationally symmetric and periodic grid to reduce computation time by several orders of magnitude overall. This had the side effect of eliminating runtime growth for larger values of r_0. In general all for loops dependent on grid size parameters are replaced by vectorized implementations (where possible) to further reduce runtime. We calculate the values of W_{ijkl} and $r_{kl,ij}$ in Python using the NumPy package, which takes very little time even for large grid sizes exceeding 100×100. We pass these values to MATLAB's built-in delayed differential equation solver (DDE23) to update θ and $\dot{\theta}$.

3 Results

We began by attempting to replicate the results shown in Figure 4 of the original paper by Jeong et al., shown below in Figure 2.

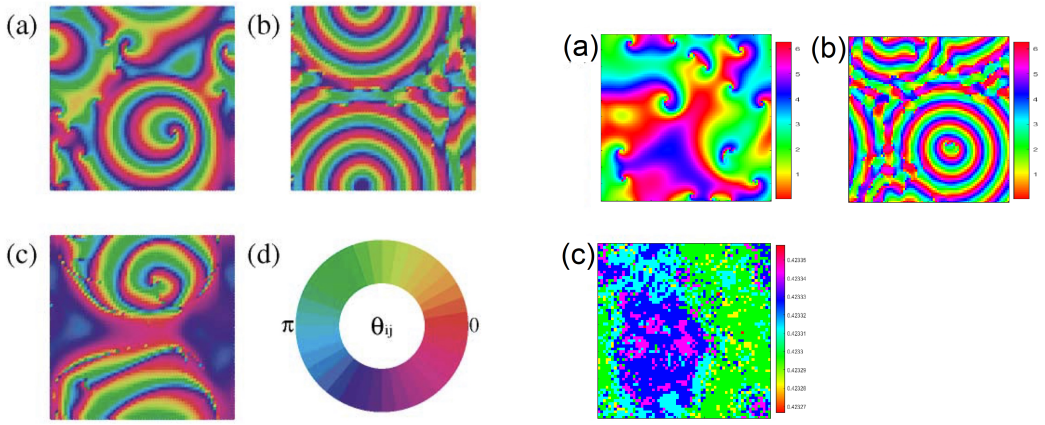

Figure 2: On the left: Results from Figure 4 of Jeong et al. On the right: Our results. Using parameters (a): $r_0 = 4$, $\frac{1}{v} = 1$, $K = 1$; (b): $r_0 = 7$, $\frac{1}{v} = 1$, $K = 0.4$; (c): $r_0 = 8$, $\frac{1}{v} = 1$, $K = 0.8$. Results for all graphs have values ranging from $(0, 2\pi)$, except for our result for (c), which has values only between $(0.42327, 0.42335)$

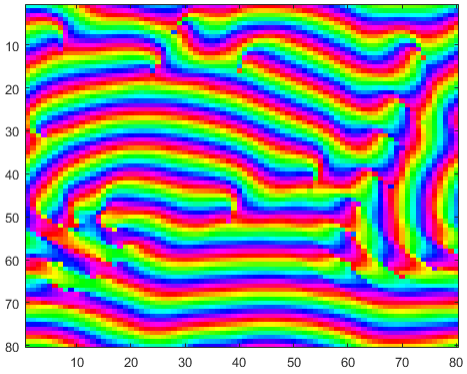

Figure 3: Our result for parameters of Jeong et al. 4b after running for some time beyond that in Figure 2.

We further explored new sets of parameters not shown in the original Jeong et al. paper, as shown below in the leftmost figure of Figure 4 below, using $r_0 = 8$, $\frac{1}{v} = 1$, $K = 0.2$. In the rightmost two images of Figure 4 below, we ran that paper's 4b and 4c respectively with initial conditions uniformly random across $(0, 2\pi)$.

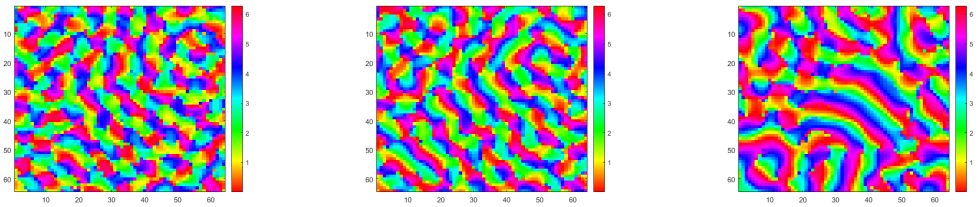

Figure 4: Our new results, all with uniformly random initial condition across $(0, 2\pi)$. Left: New parameter sets. Rightmost two images: running the parameters of Jeong et al. 4b and 4c respectively.

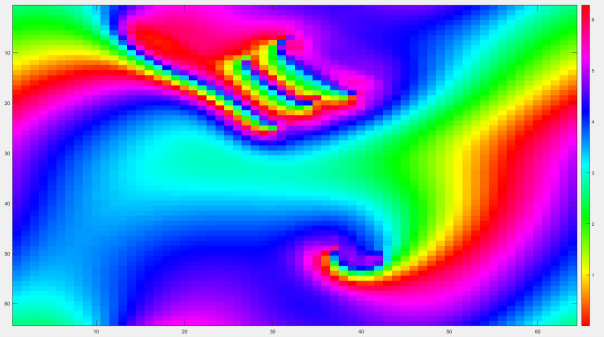

Figure 5: Using parameters from Jeong et al. Figure 4a with sparsity (33% connection probability). Initial conditions are uniformly random.

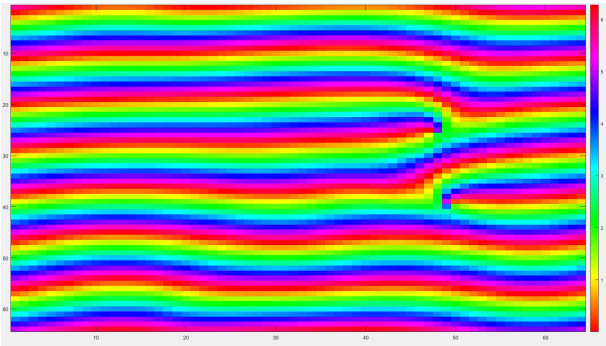

Figure 6: Using parameters from Jeong et al. Figure 4b with sparsity (33% connection probability). Initial conditions are nearly homogeneous.

Using parameters for Jeong et al. Figure 4c with 33% connection and nearly homogeneous initial conditions give nearly homogeneous results.

4 Conclusions

Overall we find the specific patterns arising from certain connectivity schemes to be replicable, but complicated and highly sensitive to initial conditions. Our attempted replication yielded similar but not identical patterns. There are several possible reasons for this; primary is that for any given parameter set, these patterns evolve and change over time. The spirals we generate in using parameter set (a) do migrate and eventually disappear over time, leaving just a couple of large spirals at some point in time. It is possible that using the same grid size and precisely the same initial conditions, we could see near exact replication.

Our result for (b) in Figure 3 closely resembles the original Figure 4b from the paper. However, letting the simulation run longer, past the point of matching circles, results in a different 'fingerprint' pattern (Figure 3). The result we attained while attempting to replicate Figure 4c from Jeong et al. suggests organization in the oscillators that may reveal spirals upon further simulation. Exact replication not only requires taking a solution snapshot at the same time, but may also be hampered by starting with different initial conditions instabilities, a smaller grid size, and instabilities in the delayed differential equation software.

Having satisfactorily replicated some of the images from the paper and a couple of new results, we looked to expand on the project by making it more biologically realistic. While there are many ways this model could be improved as discussed

above, we chose to move forward by including sparsity in the connections rather than having each neuron be fully connected to everything within its connectivity radius. Specifically, we reduced the connections of each neuron down to a random 33 percent of the original connections. Figures 5 and 6 is a figure showcase this. In Figure 5, the sparsity mixes migrating spirals with nearby traveling rolls.

The runtime is highly impacted by the calculations of the right hand side of the delayed differential equation, which bottlenecks even at small grid sizes. This is mostly due to the for loops we use. These for loops are used in place of a memory-hungry seven dimensional matrix of doubles with each axis the length of a grid axis, which would be unfeasible on our machines. This is not the only important bottleneck, however. One simulation (which took 20 hours to conclude) using the parameters of Jeong et al.'s Figure 3D demonstrated that for large values of r_0 on our machines, MATLAB's DDE23 program itself became the bottleneck. In addition, it appears that solutions degrade after a certain span of time, and degrade earlier for smaller grid sizes. This suggests that there may be a quicker algorithm which we have not implemented.

Future directions for this project include a method for defining different types of spatial patterns (rolls vs spirals etc.) and moving towards more biologically relevant set ups. This could include modeling the specific connectivity of known human circuitry, modeling different types of real neurons with different connectivity patterns and conduction speeds, etc. Furthermore, we would like to be able to find time delays that replicate spatial patterns seen during chimeric epilepsy states should those be identified in the future. The most immediate concern is increasing algorithmic efficiency in order to allow simulations with larger grid sizes and values of r_0, a concern which highlights the importance of computational efficiency in computational neuroscience.

5 Acknowledgments

We'd like to acknowledge the Neuroscience Gateway team [5] for providing computation time for this project, as well as the teaching assistants of Physics 278 for their help.

References

[1] Jeong, S.-O., Ko, T.-W., Moon, H.-T. (2002). Time-Delayed Spatial Patterns in a Two-Dimensional Array of Coupled Oscillators. Physical Review Letters, 89(15). doi: 10.1103/physrevlett.89.154104

[2] Muller, L., Chavane, F., Reynolds, J., Sejnowski, T. J. (2018). Cortical travelling waves: mechanisms and computational principles. Nature Reviews Neuroscience, 19(5), 255–268. doi: 10.1038/nrn.2018.20

[3] Ermentrout, G., Kleinfeld, D. (2001). Traveling Electrical Waves in Cortex. Neuron, 29(1), 33–44. doi: 10.1016/s0896-6273(01)00178-7

[4] Lainscsek, C., Rungratsameetaweemana, N., Cash, S. S., Sejnowski, T. J. (2019). Cortical chimera states predict epileptic seizures. Chaos, 29, 121106

[5] S Sivagnanam, A Majumdar, K Yoshimoto, V Astakhov, A Bandrowski, M. E. Martone, and N. T. Carnevale. Introducing the Neuroscience Gateway, IWSG, volume 993 of CEUR Workshop Proceedings, CEUR-WS.org, 2013.